Biosensors and Bioelectronics 26 (2011) 1959–1964

Contents lists available at ScienceDirect

Biosensors and Bioelectronics

journal homepage: www.elsevier.com/locate/bios

Impedimetric immunosensor doped with reduced graphene sheets fabricated by controllable electrodeposition for the non-labelled detection of bacteria

Yi Wan[a,b], Zhifeng Lin[a,b], Dun Zhang[a,*], Yi Wang[a], Baorong Hou[a]

[a] Key Lab of Corrosion Science, Shandong Province, Institute of Oceanology, Chinese Academy of Sciences, 7 Nanhai Road, Qingdao 266071, China
[b] Graduate School of the Chinese Academy of Sciences, 19 (Jia) Yuquan Road, Beijing 100039, China

ARTICLE INFO

Article history:
Received 31 May 2010
Received in revised form 31 July 2010
Accepted 2 August 2010
Available online 7 August 2010

Keywords:
Sulphate-reducing bacteria
Reduced graphene sheets
Electrochemical impedance spectroscopy
Chitosan
Electrodeposition

ABSTRACT

A facile, sensitive and reliable impedimetric immunosensor doped with reduced graphene sheets (RGSs) and combined with a controllable electrodeposition technique was developed for the selective detection of marine pathogenic sulphate-reducing bacteria (SRB). The morphology of RGSs and the electrochemical properties of RGSs-doped chitosan (CS) nanocomposite film were investigated by atomic force microscopy, Fourier transform infrared spectroscopy, and cyclic voltammetry (CV). Electrochemical impedance spectroscopy and CV were used to verify the stepwise assembly of the sensor system. Faradic impedance spectroscopy for charge transfer for the redox probe $Fe(CN)_6^{3-/4-}$ was done to determine SRB concentrations. The diameter of the Nyquist diagram that is equal to the charge-transfer resistance (R_{ct}) increased with increasing SRB concentration. A linear relationship between R_{ct} and SRB concentration was obtained in the SRB concentration range of 1.8×10^1 to 1.8×10^7 cfu/ml. The impedimetric biosensor gave a distinct response to SRB, but had no obvious response to *Vibrio angillarum*. It showed a high selectivity for the detection of the pathogen. Based on a combination of the biocompatibility of CS and good electrical conductivity of RGSs, a nanocomposite film with novel architecture was used to immobilize biological and chemical targets and to develop a new type of biosensor.

1. Introduction

Conventional methods for monitoring microbial sulphate-reducing bacteria (SRB) populations, such as the most probable number (MPN) method (Abd-El-Malek and Rizk, 1958), involve a pre-enrichment step or a selective enrichment step, followed by a biochemical test. The sophisticated series of assays required can take up to half a month to complete. A variety of protocols have been reported for detecting SRB. These include the improved MPN method (Stilinovic and Hrenovic, 2004; Vester and Ingvorsen, 1998), the enzyme-linked immunosorbent assay (Gibson and Gibson, 1988; Lillebaek, 1995; Smith, 1982), and pertinent molecular techniques, such as polymerase chain reaction (Menert et al., 2004; Zhu et al., 2006) or fluorescence in situ hybridization (Lücker et al., 2007). Though promising, these techniques are still in the development phase and several problems may occur when they are used in situ and in real time. Rapid approaches for pathogen detection are essential to food safety, prevention of environmental contamination, and clinical diagnosis of food poisoning and food-borne and water-borne diseases.

Biosensors have emerged as extremely useful tools for pathogenic detection. Various sensitive, reliable and rapid methods have been reported for the determination and monitoring of microorganisms, including surface plasma resonance (Subramanian et al., 2006; Taylor et al., 2006), flow cytometry (Karo et al., 2008), epifluorescence microscopy (Brewster et al., 1996), quartz crystal microbalance (Hong et al., 2009; Poitras and Tufenkji, 2009), mass spectrometry (Lin et al., 2005), and insulator-based dielectrophoresis (Betts, 1995). Other methods use gold- or silver-nanoparticles or quantum dots as detecting mediators combined with electrochemical techniques (Kuo et al., 2008; Singh et al., 2009; Xue et al., 2009), and still others selectively detect cellular compounds such as ATP (Cheng et al., 2009), nucleic acids (Meyer et al., 2007), and whole cells with specific antigens or typical structures of the carbohydrate domain (Shen et al., 2007).

Among the available biosensor platforms, the impedimetric sensor has been applied to measure changes at electrode interfaces for recognition of biological and chemical substances. Electrochemical impedance spectroscopy (EIS) is usually performed by applying a small excitation signal as a function of the frequency. Owing to its unique advantages, an impedimetric sensor has been applied in a broader range of applications in biological studies, such as in the detection and kinetics study of protein or antigen (Barton et al., 2008; Huang et al., 2008; Li et al., 2008; Rezaei et al., 2009; Tsekenis et al., 2008a; Xiao et al., 2007), sensing of DNA

* Corresponding author. Tel.: +86 532 82898960; fax: +86 532 82898960.
E-mail address: zhangdun@ms.qdio.ac.cn (D. Zhang).

0956-5663/$ – see front matter © 2010 Elsevier B.V. All rights reserved.
doi:10.1016/j.bios.2010.08.008

for specific recognition (Keighley et al., 2008; Li et al., 2004; Wang et al., 2008), assessment of cytotoxicity and antibiotics (La Belle et al., 2007; Tsekenis et al., 2008b) and detection of pathogenic bacteria (Yang and Bashir, 2008). In earlier biosensors, specific antibody or lectin was directly immobilized onto the surface of an electrode as the target for recognizing pathogenic bacteria (Gamella et al., 2009; Maalouf et al., 2007; Mantzila et al., 2008; Ruan et al., 2002). Low-cost and versatile screen printed carbon electrode arrays have recently been used as base transducers to immobilize the lytic phage, which acts as a recognition element for the detection of pathogen by impedance measurement (Shabani et al., 2008). In addition, interdigitated microelectrodes were also applied as impedance measurement sensors for the quantitative detection of viable pathogen in selective media and milk samples (Varshney and Li, 2007, 2009; Yang et al., 2004). Our group recently reported on the impedimetric immunosensor based on an agglutination assay on a planar electrode and antibody recognition on a 3D Ni foam substrate for the detection of bacterial cell and the monitoring of SRB population (Wan et al., 2009, 2010).

In recent years, reduced graphene sheets (RGSs), which are monolayers of carbon atoms packed into a dense honeycomb crystal structure, have attracted attention from scientific communities. Their unique nanostructure and properties, such as high surface area, high conductivity, and low manufacturing cost, give it potential applications as a catalyst support for electron transfers involved in biosensors. For example, polyethylenimine-functionalized graphene ionic liquid nanocomposites (Shan et al., 2009) or RGSs-doped chitosan complex with a conductive architecture (Kang et al., 2009; Wu et al., 2010) are potential materials for glucose biosensors. Their electronic properties and biocompatibility for graphene-based composites results in a direct electron transfer of glucose while maintaining good bioactivity. Graphene nanosheets decorated with Au and Pt were also considered as immobilization matrices for glucose biosensors (Baby et al., 2010; Shan et al., 2010; Wu et al., 2009). Moreover, chemically RGSs have been used as biosensor platforms for electrochemical sensing of all four DNA bases in both single-stranded and double-stranded DNA without the need of a pre-hydrolysis step. It has also been used in the detection of a single-nucleotide polymorphism site for short oligomers without the need for labelling processes (Zhou et al., 2009).

The application of the biocompatible CS polymer in the development of biosensors is still limited because of its low conductive properties. As such, Au nanoparticles, carbon nanotubes, and graphene were introduced into a hybrid film to enhance the electrical conductivity of CS-based nanocomposite films and increase the sensitivity of the electrochemical sensor. A conventional method for the fabrication of nanoparticle-doped CS-based nanocomposite film is simply coating a mixture of nanoparticles and CS on the electrode (Wu et al., 2010). However, the nanocomposite-coated film usually shows a heterogeneous microstructure, resulting to biological and chemical molecule detachment and poor biosensor stability. Compared to the traditional protocol for conductive film fabrication, the electrogeneration approach is simple, controllable, and reproducible. For example, Qiu et al. reported a simple and controllable electrodeposition method for the fabrication of a homogenous CS-based nanocomposite film that exhibits good analytical performance toward the quantification of glucose (Qiu et al.,2009). Hao et al. used nitric acid-treated carbon nanofibres (CNF) as electron conductors in a controllable electrodeposition process using soluble CNF-doped CS colloidal solution for the preparation of a sensitive biosensor for cytosensing (Hao et al., 2007).

In this study, we developed a RGSs-doped impedimetric immunosensor through a controllable electrodeposition method using soluble RGSs-doped CS solution for the facile and rapid detection of SRB. We used RGSs as electron conductors to obtain good analytical performance, namely, sensitivity, selectivity, and stability, of the biosensor towards the detection of pathogen. The morphology and electrochemical property of the fabricated RGSs-doped CS film were characterized by atomic force microscopy (AFM), Fourier transform infrared (FT-IR) spectroscopy, and cyclic voltammetry (CV). The microbial population of SRB bound to the antibody on the surface of the electrode was estimated by fluorescence microscopy.

2. Materials and methods

2.1. Chemicals and solutions

For the synthesis of RGSs, nature graphite powder (99.99%) was purchased from Beijing Chemical Company. Rabbit antibody against SRB was from Abmart Inc. (Shanghai, China). CS (95% deacetylation) was from Sinopharm Chemical Reagent Co., Ltd. Bovine serum albumin (BSA), Fluorescein isothiocyanate (FITC), *N*-hydroxisuccinimide (NHS), 1-ethyl-3[3-dimethylaminopropyl] carbodiimide hydrochloride (EDC) were obtained from Sigma (USA). Other chemicals used in this paper were purchased from Sinopharm Chemical Reagent Co., Ltd, China. All solutions were prepared using Milli-Q water (Milli-Q, USA). All chemicals were of analytical grade and used without further purification.

A series of chemicals, including magnesium sulphate, ammonium chloride, sodium sulphate, calcium chloride, dipotassium hydrogen phosphate, sodium hydroxide, sodium lactate, and yeast extract, were used to prepare the modified Postgate's culture medium.

2.2. Bacterial cultivation

Seed bacteria were isolated from marine mud collected from the Bohai Sea, China. Pure SRB culture was grown in modified Postgate's medium at 30 °C for 4 d. Bacterial cells were then isolated through centrifugation (6000 rpm, 20 min) and then rinsed thrice with PBS. Before measurements, SRB samples were stored in the refrigerator at 4 °C to slow down growth. The culture was serially diluted with physiological saline solution and viable cell number was determined by the most probable number (MPN) method according to the American Society of Testing materials standard D4412-84. The MPN method, otherwise known as the method of Poisson zeroes, is a method of getting quantitative data on concentrations of discrete items from positive data. To increase the statistical accuracy of this test, the standard MPN procedure used a minimum of five tubes per dilution. After incubation, the pattern of the positive tubes was noted, and a standardized MPN table was consulted to determine the most probable number of microorganisms per unit volume of the original sample. *Vibrio anguillarum* was contributed by Dr. Zhaolan Mo and used as control.

2.3. Preparation of RGSs–CS film and fabrication of sensor

Graphene oxide (GO) was prepared from graphite according to Hummers method (Hummers and Offeman, 1958). Graphite was oxidized by concentrated H_2SO_4 and $KMnO_4$ to produce pre-oxide graphite. Pre-oxide graphite was then re-oxidized to GO by H_2O_2. Then, GO was delaminated into GO sheets by sonication for 30 min. Hydrazine was used to reduce GO sheets, and finally, blank RGSs were obtained by filtration and drying in vacuum.

CS is soluble in acidic solution, in which it behaves as a cationic polyelectrolyte. A 1 wt% CS stock solution was prepared by dissolving CS flakes in 1% acetic acid solution at 40 °C. The mixture was cooled to room temperature, and its pH was adjusted to 6.10 using 1 M NaOH. The CS solution was filtered and stored in a refrigerator

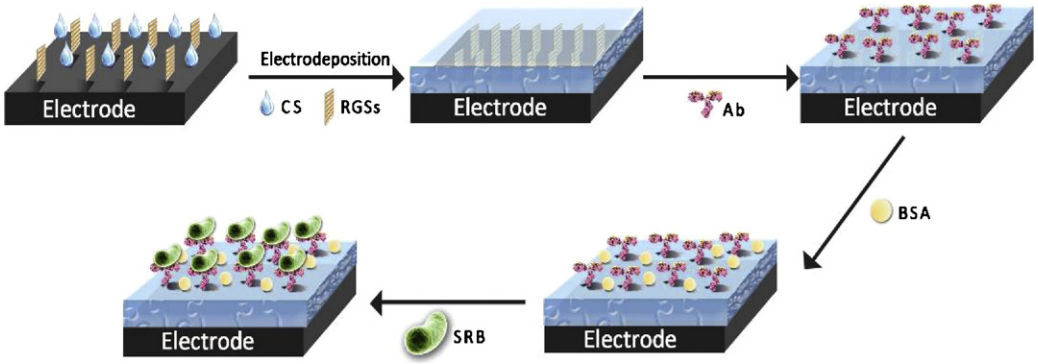

Scheme 1. Electrogeneration of RGSs–CS film and impedance sensor for the detection of SRB.

(4 °C). The RGSs were suspended in CS solution (0.1–0.6 mg mL^{-1}) for subsequent experiments.

Before use, glassy carbon (GC) electrodes were polished using a polishing cloth (CHI Inc.) with small particles (1.0 and 0.05 mm) of Al_2O_3 slurry, rinsed with water, and then ultrasonicated in ethanol and doubly distilled water. The electrogeneration process was performed by immersing GC electrodes in a RGSs–CS solution at −2.5 V for 300 s. The pretreated electrodes were then rinsed with Milli-Q water and air-dried. The Ab/RGSs–CS-modified GC electrodes were fabricated by immersing the freshly made RGSs–CS/GC electrode, which was activated using 1% glutaraldehyde solution, into a solution containing anti-SRB antibody (5 mg mL^{-1}) for 10 h in 4 °C. The electrode was then rinsed with water to remove the physically absorbed antibody prior to use in the following procedure. As shown in Scheme 1, 1% BSA was used to block the non-specific sites on the surface of the functionalized electrode. Finally, a series of SRB solutions (10 μl) were added and incubated for 1 h. After each step, the electrode was rinsed thoroughly with Milli-Q water and then dried with a stream of nitrogen.

2.4. Electrochemical measurements

Electrochemical measurements were made using a CHI430D conventional three electrode system (CH Instruments, Inc., Shanghai) that included a platinum wire as a counter electrode and an Ag/AgCl (3 M KCl) wire as the reference electrode. Experiments were performed at room temperature with a 3.0 mm diameter glassy carbon disk working electrode. The electrochemical properties of RGSs–CS composite film, bacteria voltammetric behaviour, and detection were performed using CV. EIS was used to characterize the stepwise modification process of the functionalized electrodes and to count the bacterial population. It was conducted in 1 M KCl in the presence of the redox probe with 10 mM $K_3Fe(CN)_6$ at the open circuit potential vs. Ag/AgCl (3 M KCl) and an alternating potential with an amplitude of 10 mV at the frequency range of 0.1 Hz–100 kHz. The experiments, such as bacteria count using MPN, sensor fabrication and RGSs–CS film preparation, were done in triplicate, and the means of the results were presented with the standard deviations.

3. Results and discussion

3.1. Synthesis of RGSs and RGSs–CS film

Fig. 1S shows the atomic force microscopy (AFM) (Nanoscope IIIa, Digital Instruments, USA) data of the synthesized RGSs in water. These were almost entirely like monolayer sheets with a thickness of ca. 0.7 nm and lateral dimensions of several hundred of nanometers. The nanosize sheets contained an amount of open graphitic edge planes, which give it outstanding thermal, mechanical, and electrochemical properties (Geim, 2009).

A mixture containing graphene and chitosan was sonicated for 1 h. Graphene was well-dispersed in the aqueous chitosan solution, forming a stable colloidal solution with a small amount of graphene precipitated overnight. The carboxyl and hydroxyl groups of graphene could interact with the reactive amino and hydroxyl functional group of CS to form a dispersed graphene-CS colloidal solution.

When less than −1.4 V was applied, the hydrogen ion in the graphene–CS colloidal solution was reduced to hydrogen gas in the vicinity of the electrode interface, resulting in an increase in pH value. Dissolved CS with incorporated graphene sheets were electrodeposited on the surface of the electrode to form a hydrogel structure, which occurred due to the deprotonation of the amine group as the pH gradually increased (Hao et al., 2007). As the electrochemical reduction of hydrogen ions continually progresses, more insoluble graphene–CS mixtures were deposited on the surface of the electrode to form a hydrogel network (shown in Fig. 5S). The evolved hydrogen molecules could function as a dynamic template for the formation of a porous hydrogel network (Qiu et al., 2009).

3.2. Optimization and characterization of RGSs–CS film

The impedimetric immunosensor is based on the electrochemical response of the redox probe in the form of graphene-doped CS films. Fig. 2S shows the change in the peak current obtained from the preparation of graphene-doped CS film under different assay conditions, including graphene concentration, electrodeposition potential, and electrodeposition time. The film was prepared using 5 mM $[Fe(CN)_6]^{3-/4-}$ redox probe in PBS (pH = 7.4) at scan rate of 100 mV s^{-1}. With increasing concentrations of graphene, from 0 to 0.3 mg mL^{-1}, in the CS solution, the peak current response increased and then decreased sharply (Fig. 2SA). The co-aggregation of high concentration graphene resulted in a reduction of the conductive property of the graphene-doped CS film. In addition, excessive graphene sheets as an immobilization platform for antibodies adversely affected antibody bonding. Therefore, the optimum concentration of graphene (0.3 mg mL^{-1}) was chosen in the subsequent experiments.

Electrodeposition potential and time controlled the thickness of the graphene-doped CS film. This, in turn, affected the immobilization of anti-SRB antibody on the fabricated film and the electron transfer of the redox probe. The electrodeposition potential could contribute to a change in the peak current signal. The influence of the electrodeposition potential on the response was investi-

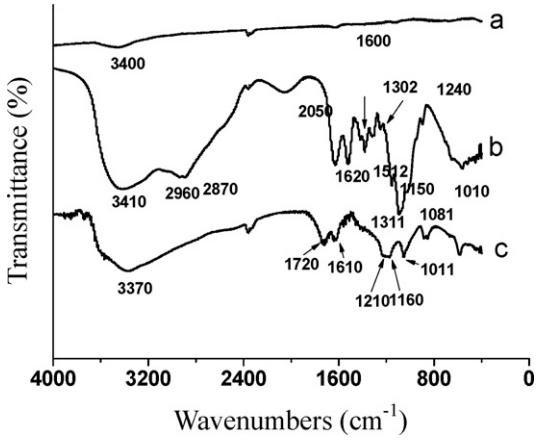

Fig. 1. Infrared spectra of RGSs (a), CS (b), and RGSs-doped CS powder (c).

gated to optimise the assay conditions. As seen in Fig. 2SB, there was a marked decrease in peak current signal, and a stable state was maintained from −2.0 to −3.0 V. When the electrodeposition potential was more negative than −3.0 V, an unstable and uneven graphene-doped CS film was found to be unfavourable to the immobilization of biological and chemical micromolecules. Therefore, the optimised electrodeposition potential was −2.5 V.

The electrodeposition time was studied from 150 to 400 s. The results (Fig. 2SC) showed the dependence of the electrodeposition time and the peak current response when other assay conditions were maintained. As the deposition time increased, the peak current response rapid decreased and then levelled off until a stable platform was reached after 250 s. This is due that it is difficult for the reduced graphene sheets in high concentration to bind chemically with CS. In other word, the loose and instability nanocomposite film was electrodeposited on the surface of electrode resulted in a reduction of the conductive property of the graphene-doped CS film. An electrodeposition time of 300 s was selected to effectively fabricate the conductive nanocomposite film because a relatively stable signal was observed at this period.

The metastable behaviour of the electrodeposited nanocomposite film with sequential times was also an important factor for sensor performance. With an increasing time the response of peak current decreased sharply and approached a stable value after 12 h. In this work, the fabrication time of impedimetric sensor including antibody modification, BSA blocking and SRB absorption is more than 12 h (shown in Fig. 2SD).

The FT-IR spectra of graphene, CS, and graphene-doped CS film were obtained from the surface of the electrocoated electrode by reflectance-FT-IR measurements. The absorption bands of each spectrum are given in Fig. 1. Peaks of CS at around 1150, 1081 and 1010 cm^{-1} were due to the assigned saccharine structure. A strong characteristic peak for acylamide was observed at 1620 cm^{-1}, and both methyl characteristic peaks of acetylated chitosan were observed at 2870 and 2960 cm^{-1}. The spectrum of graphene only showed the characteristics of the hydroxyl group at 3400 cm^{-1} and carboxyl group at 1600 cm^{-1}. For the electrodeposited graphene-doped CS film, methyl peaks appeared at 2870 and 2960 cm^{-1} and then disappeared due to the hydrolysis of acetyl groups. Peaks for other functional groups could also be observed but peaks for hydroxyl, carboxylate, and carboxyl groups are all shifted. Thus, the active group interaction between carboxyl, hydroxyl, and amine groups or the formation of hydrogen bonds for CS and graphene resulted in signal shifts in the FT-IR spectrum. This result indicated that there is the chemical binding between CS and graphene in film via electrodeposition technique.

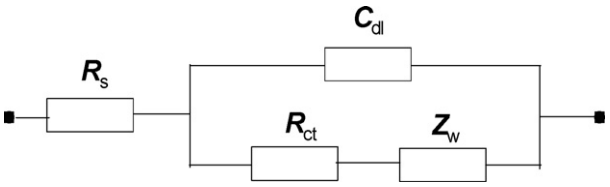

Fig. 2. Randle equivalent circuit for the impedance spectra.

3.3. Fabrication of sensor

The CV of soluble electroactive species provides a convenient tool to monitor changes in electrode behaviour after each assembly step. Fig. 3S (see the Supplementary Material) shows the CVs of the 5 mM $[Fe(CN)_6]^{3-/4-}$ redox probe in PBS (pH = 7.4), recorded at a scan rate of 100 mV s^{-1} for the bare GC electrode: (a) RGSs-doped CS/GC: (b) Ab/RGSs-doped CS/GC: (c) BSA/Ab/RGSs-doped CS/GC (d) and after formation of the immunochemical complex at the surface of the BSA/Ab/RGSs-doped CS/GC electrode incubated with 2.1×10^7 cfu/ml SRB culture for 1 h. After the bare GC electrode was electrodeposited with a graphene-doped CS film, the redox probed exhibited low permeability, and the response current decreased. When anti-SRB antibody molecules were immobilized on the graphene-doped CS film via electrostatic interaction between amine and carboxyl groups, the penetration of the redox probe was reduced. Therefore, the response current decreased. The immunochemical reaction of the SRB cell with the antibody film was accompanied by a decrease in the Faradic response and showed that the electron-transfer kinetics of the redox probe was obstructed.

3.4. Impedance sensor for SRB

As a sensitive and reliable tool, the impedance technique has been applied in biosensors to measure the change of electrode interface based on biological and chemical molecule recognition. The EIS spectra are often simulated with the modified Randles circuit (shown in Fig. 2). In particular, the modified equivalent circuit takes on a mixed electron-transfer kinetics and a diffusion controlled model, where the ohmic resistance of the electrolyte solution between the modified working electrode and the Ag/AgCl reference electrode is represented by a resistance R_s, C_{dl} is the double layer capacitance, and R_{ct} is the charge-transfer resistance of the redox couple. The Warburg impedance (Z_w) with semi-infinite diffusion mechanism in the measurement system arises from the diffusion resistance of the Fe $(CN)^{-3/-4}$ redox probe, between the bulk solution and the interface of modified work electrode. For Faradic impedance measurement, the R_{ct} is the most sensitive and straightforward parameter that can be used to characterize the events occurring on the surface of the work electrode via the diameter of the semicircle in the Nyquist plots because the two elements, R_s and Z_w, are almost not influenced by chemical transformations of the electrode surface. Moreover, the variation in C_{dl} is unnoticeable compared to the change in R_{ct}. In addition, R_{ct} is directly extracted from the Nyquist plots based on the intercept of the semicircle with the real axis.

It is very attractive for affinity capture of specific bacteria with antibody-modified electrode. The specificity of the biosensor was investigated in relation to other bacteria, such as *V. anguillarum*, a Gram-negative marine pathogenic bacteria. Fig. 3 indicates that there is a minor change in R_{ct} response of the antibody-modified electrode immersed in *V. anguillarum* (1.8×10^7 cfu/ml) for 1 h. Meanwhile, we have also investigated the influence of sensor signal of different concentration *V. anguillarum* to functionalized electrode. When the bacterial concentration is less than

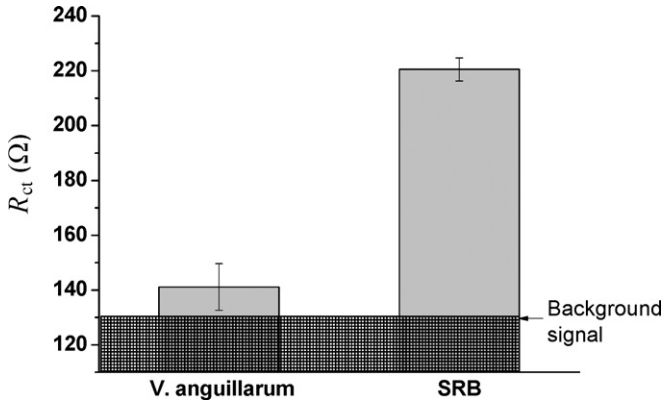

Fig. 3. Comparison of response of RGSs-doped impedimetric immunosensor to 1.8×10^7 cfu/ml sulphate-reducing bacteria (SRB) or 2.1×10^7 cfu/ml *Vibrio anguillarum*.

1.8×10^5 cfu/ml, there is almost no change in R_{ct} response. When the bacterial concentration is more than 1.8×10^5 cfu/ml, there is minor change in R_{ct} response (less than 20 Ω). When the antibody-modified electrode was immersed in SRB (1.8×10^7 cfu/ml) for 1 h, the R_{ct} response increased compared to the blank sample. Heterogeneous bacteria can be detected and discriminated by changing the magnitudes of R_{ct}.

Seven SRB concentrations from 1.8×10^1 to 1.8×10^7 cfu/ml were prepared by serial dilution in PBS. A series of SRB were added on the surface of the functionalized electrode. Fig. 4A shows the Faradic impedance spectra obtained on the graphene-doped electrodes prepared with different SRB concentrations. The diameter of the Nyquist plots increased regularly with the increase of the SRB concentrations, indicating that SRB were absorbed onto the surface of the graphene-doped electrode to produce a packed film that showed electron transfer for the redox probe.

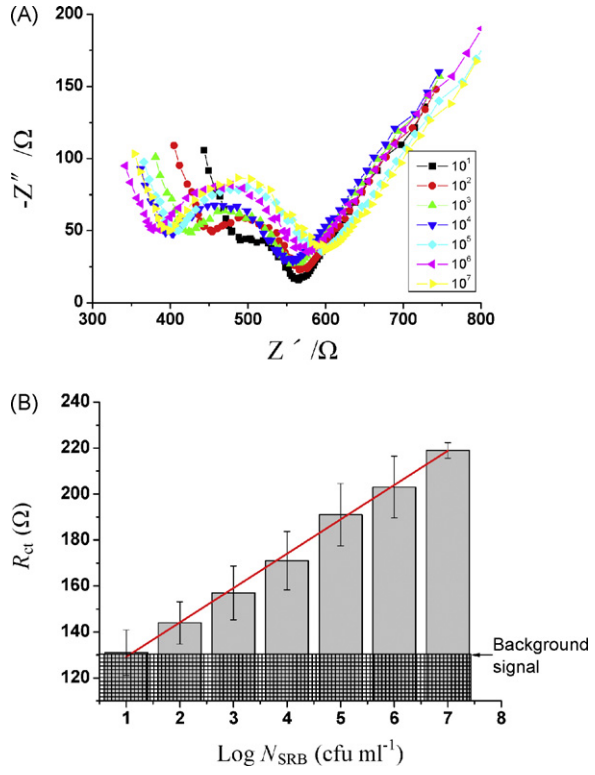

Fig. 4. Impedance spectra (A) and calibration curve (B) between the impedimetric responses and concentrations of sulphate-reducing bacteria (SRB).

This is an interesting result that the most sensitive variation of signal in our graphene-doped impedimetric sensor appeared in the high frequency domain rather than the low frequency for conventional impedimetric sensor. We obtained an interesting result may be due to good electrochemical properties of graphene sheets resulting in the variation of impedance signal in the high frequency domain. The results for the graphene-doped impedimetric immunosensor assay showed that the concentration of bacteria and the ΔR_{ct} response were highly correlated (Fig. 4B). A linear relationship between ΔR_{ct} response and the logarithm of the bacterial concentration was obtained for concentrations ranging from 1.8×10^2 to 1.8×10^7 cfu/ml, with a slope of 14.94 and a correlation coefficient of 0.99 ($R_{ct} = 14.94 \log N_{SRB} + 114.2$). The ΔR_{ct} value in the graphene-undoped impedimetric immunosensor assay almost did not vary with the logarithmic value of the SRB concentration over seven orders of magnitude. However, the graphene-undoped film still showed a low sensitivity for electron transfer and weak signal change for different bacteria concentration from 1.8×10^1 to 1.8×10^7 cfu/ml. Results indicated that the sensing platform doped graphene can improve the sensitivity and linear range of impedimetric sensor for the detection of bacteria.

Various methods have been developed for the detection of SRB, including MPN, biochemical tests, and polymerase chain reaction. Although these techniques for pathogen detection are sufficiently sensitive and selective, most have several disadvantages including being time-consuming (e.g., MPN), cost-intensive (e.g., specific enzyme-labelled antibodies), or technically complex (e.g., DNA analysis). Recently, our group have worked in the research line of the impedimetric immunosensor based on self-assembled monolayer immobilized with lectin and antibody for the detection of bacterial cell and the monitoring of SRB population (Wan et al., 2009, 2010). Compared with methods for the detection of SRB, the typical impedimetric sensor based on self-assembled monolayer require extensive and prolonged modification processes (more than 12 h), unlike the electrodeposited technique, which can be used directly to fabricate the sensing platform in a short time (less than 10 min).

3.5. Fluorescence microscopy

The direct detection of microorganisms and their traces by fluorescence microscopy is one of the most promising techniques to obtain decisive evidence for the presence of bacteria cell. This technique offers high sensitivity and spatial information with a high resolution. Serially diluted solutions of SRB were incubated with an antibody-functionalized graphene-doped CS film platform, washed to remove unbound SRB, stained with FITC dyes, and imaged using fluorescence microscopy to estimate the number of bacteria. Results (Fig. 4S) showed that fluorescence-stained clusters of bacterial cells can be observed with as little as 10^2 cfu/ml. This is similar to the detection limit that is observed using the impedance method.

4. Conclusion

Low-cost, versatile, and robust RGSs-doped impedimetric immunosensors combined with controllable electrodisposition was fabricated for SRB detection. The proposed sensor for SRB detection shows good fabrication reproducibility and measurement precision. The synthesized RGSs mostly appeared as monolayer sheets in water. These had lateral dimensions of several hundred nanometers, as observed by AFM. The FT-IR results indicated that the interaction between the carboxyl group of RGSs and the amine group of CS resulted in the formation of the nanocom-

posite film. The nanocomposite film with a novel architecture was used to immobilize the pathogenic bacteria and to pave the way for the application of RGSs in biosensors.

Acknowledgements

This work was supported by the National Natural Science Foundation of China (Grant No. 40876041), the National Key Technology R&D Program of China (Grant No. 2007BAB27B01), Science & Technology Basic Research Program of Qingdao (Grant No. 09-1-3-16-jch).

Appendix A. Supplementary data

Supplementary data associated with this article can be found, in the online version, at doi:10.1016/j.bios.2010.08.008.

References

Abd-El-Malek, Y., Rizk, S.G., 1958. Nature 182 (4634), 538–1538.
Baby, T.T., Aravind, S.S.J., Arockiadoss, T., Rakhi, R.B., Ramaprabhu, S., 2010. Sens. Actuat. B 45 (1), 71–77.
Barton, A.C., Davis, F., Higson, S.P.J., 2008. Anal. Chem. 80 (24), 9411–9416.
Betts, W.B., 1995. Trends Food Sci. Technol. 6 (2), 51–58.
Brewster, J.D., Gehring, A.G., Mazenko, R.S., Van Houten, L.J., Crawford, C.J., 1996. Anal. Chem. 68 (23), 4153–4159.
Cheng, Y., Liu, Y., Huang, J., Li, K., Zhang, W., Xian, Y., Jin, L., 2009. Talanta 77 (4), 1332–1336.
Gamella, M., Campuzano, S., Parrado, C., Reviejo, A.J., Pingarron, J.M., 2009. Talanta 78 (4–5), 1303–1309.
Geim, A.K., 2009. Science 324 (5934), 1530–1534.
Gibson, S.A.W., Gibson, G.R., 1988. Lett. Appl. Microbiol. 7 (2), 33–35.
Hao, C., Ding, L., Zhang, X., Ju, H., 2007. Anal. Chem. 79 (12), 4442–4447.
Hong, S.-R., Choi, S.-J., Jeong, H.D., Hong, S., 2009. Biosens. Bioelectron. 24 (6), 1635–1640.
Huang, Y., Bell, M.C., Suni, I.I., 2008. Anal. Chem. 80 (23), 9157–9161.
Hummers, W.S., Offeman, R.E., 1958. J. Am. Chem. Soc. 80 (6), 1339–11339.
Kang, X., Wang, J., Wu, H., Aksay, I.A., Liu, J., Lin, Y., 2009. Biosens. Bioelectron. 25 (4), 901–905.
Karo, O., Wahl, A., Nicol, S.B., Brachert, J., Lambrecht, B., Spengler, H.P., Nauwelaers, F., Schmidt, M., Schneider, C.K., Muller, T.H., Montag, T., 2008. Clin. Chem. Lab. Med. 46 (7), 947–953.
Keighley, S.D., Estrela, P., Li, P., Migliorato, P., 2008. Biosens. Bioelectron. 24 (4), 906–911.
Kuo, Y.C., Wang, Q., Ruengruglikit, C., Yu, H.L., Huang, Q.R., 2008. J. Phys. Chem. C 112 (13), 4818–4824.
La Belle, J.T., Bhavsar, K., Fairchild, A., Das, A., Sweeney, J., Alford, T.L., Wang, J., Bhavanandan, V.P., Joshi, L., 2007. Biosens. Bioelectron. 23 (3), 428–431.
Li, C.-Z., Liu, Y., Luong, J.H.T., 2004. Anal. Chem. 77 (2), 478–485.
Li, X., Shen, L., Zhang, D., Qi, H., Gao, Q., Ma, F., Zhang, C., 2008. Biosens. Bioelectron. 23 (11), 1624–1630.
Lillebaek, R., 1995. Appl. Environ. Microbiol. 61 (9), 3436–3442.
Lin, Y.-S., Tsai, P.-J., Weng, M.-F., Chen, Y.-C., 2005. Anal. Chem. 77 (6), 1753–1760.
Lücker, S., Steger, D., Kjeldsen, K.U., MacGregor, B.J., Wagner, M., Loy, A., 2007. J. Microbiol. Methods 69 (3), 523–528.
Maalouf, R., Fournier-Wirth, C., Coste, J., Chebib, H., Saikali, Y., Vittori, O., Errachid, A., Cloarec, J.-P., Martelet, C., Jaffrezic-Renault, N., 2007. Anal. Chem. 79 (13), 4879–4886.
Mantzila, A.G., Maipa, V., Prodromidis, M.I., 2008. Anal. Chem. 80 (4), 1169–1175.
Menert, A., Paalme, V., Juhkam, J., Vilu, R., 2004. Thermochim. Acta 420 (1–2), 89–98.
Meyer, M.H.F., Stehr, M., Bhuju, S., Krause, H.-J., Hartmann, M., Miethe, P., Singh, M., Keusgen, M., 2007. J. Microbiol. Methods 68 (2), 218–224.
Poitras, C., Tufenkji, N., 2009. Biosens. Bioelectron. 24 (7), 2137–2142.
Qiu, J.-D., Wang, R., Liang, R.-P., Xia, X.-H., 2009. Biosens. Bioelectron. 24 (9), 2920–2925.
Rezaei, B., Khayamian, T., Majidi, N., Rahmani, H., 2009. Biosens. Bioelectron. 25 (2), 395–399.
Ruan, C., Yang, L., Li, Y., 2002. Anal. Chem. 74 (18), 4814–4820.
Shabani, A., Zourob, M., Allain, B., Marquette, C.A., Lawrence, M.F., Mandeville, R., 2008. Anal. Chem. 80 (24), 9475–9482.
Shan, C., Yang, H., Han, D., Zhang, Q., Ivaska, A., Niu, L., 2010. Biosens. Bioelectron. 25 (6), 1504–1508.
Shan, C., Yang, H., Song, J., Han, D., Ivaska, A., Niu, L., 2009. Anal. Chem. 81 (6), 2378–2382.
Shen, Z., Huang, M., Xiao, C., Zhang, Y., Zeng, X., Wang, P.G., 2007. Anal. Chem. 79 (6), 2312–2319.
Singh, A.K., Senapati, D., Wang, S.G., Griffin, J., Neely, A., Candice, P., Naylor, K.M., Varisli, B., Kalluri, J.R., Ray, P.C., 2009. ACS Nano 3 (7), 1906–1912.
Smith, A.D., 1982. Arch. Microbiol. 133 (2), 118–121.
Stilinovic, B., Hrenovic, J., 2004. Folia Microbiol. 49 (5), 513–518.
Subramanian, A., Irudayaraj, J., Ryan, T., 2006. Biosens. Bioelectron. 21 (7), 998–1006.
Taylor, A.D., Ladd, J., Yu, Q.M., Chen, S.F., Homola, J., Jiang, S.Y., 2006. Biosens. Bioelectron. 22 (5), 752–758.
Tsekenis, G., Garifallou, G.-Z., Davis, F., Millner, P.A., Gibson, T.D., Higson, S.P.J., 2008a. Anal. Chem. 80 (6), 2058–2062.
Tsekenis, G., Garifallou, G.-Z., Davis, F., Millner, P.A., Pinacho, D.G., Sanchez-Baeza, F., Marco, M.P., Gibson, T.D., Higson, S.P.J., 2008b. Anal. Chem. 80 (23), 9233–9239.
Varshney, M., Li, Y.B., 2007. Biosens. Bioelectron. 22 (11), 2408–2414.
Varshney, M., Li, Y.B., 2009. Biosens. Bioelectron. 24 (10), 2951–2960.
Vester, F., Ingvorsen, K., 1998. Appl. Environ. Microbiol. 64 (5), 1700–1707.
Wan, Y., Zhang, D., Hou, B., 2009. Talanta 80 (1), 218–223.
Wan, Y., Zhang, D., Wang, Y., Hou, B., 2010. Electrochem. Commun. 12 (2), 288–291.
Wang, Y., Li, C., Li, X., Li, Y., Kraatz, H.-B., 2008. Anal. Chem. 80 (6), 2255–2260.
Wu, H., Wang, J., Kang, X.H., Wang, C.M., Wang, D.H., Liu, J., Aksay, I.A., Lin, Y.H., 2009. Talanta 80 (1), 403–406.
Wu, J.-F., Xu, M.-Q., Zhao, G.-C., 2010. Electrochem. Commun. 12 (1), 175–177.
Xiao, Y., Li, C.M., Liu, Y., 2007. Biosens. Bioelectron. 22 (12), 3161–3166.
Xue, X.H., Pan, J., Xie, H.M., Wang, J.H., Zhang, S., 2009. Talanta 77 (5), 1808–1813.
Yang, L., Bashir, R., 2008. Biotechnol. Adv. 26 (2), 135–150.
Yang, L.J., Li, Y.B., Griffis, C.L., Johnson, M.G., 2004. Biosens. Bioelectron. 19 (10), 1139–1147.
Zhou, M., Zhai, Y., Dong, S., 2009. Anal. Chem. 81 (14), 5603–5613.
Zhu, X.Y., Modi, H., Ayala, A., Kilbane, J.J., 2006. Corrosion 62 (11), 950–955.